# THEORETICAL STUDIES OF LOWER HYBRID CURRENT DRIVE AND ION-CYCLOTRON HEATING IN TOKAMAKS

PPPL--2144

DE85 008712

by

F. W. Perkins, E. J. Valeo, D. C. Eder,
D. Q. Hwang, F. Jobes, and C. K. Phillips,

Plasma Physics Laboratory, Princeton University
P.O. Box 451, Princeton, NJ 08544

D.G. Swanson,[†] K. Hizanidis,[††] V. Krapchev,[††]
D. Hewett,[††], A. Bers[††], G. D. Kerbel,[†††] M. G. Mc Coy,[†††]
J. Killeen,[†††] R. W. Harvey, [††††] and S. C. Chiu[††††]

Abstract

A computational model for PLT lower hybrid current drive and ramp-up experiments combines a parallel velocity Fokker-Planck treatment of lower hybrid current drive with minor radius flux diffusion and toroidal ray-tracing wave propagation. Computational and experimental results are in good accord. Analytic solutions of the two-dimensional velocity space ($v_\perp$, $v_\parallel$) diffusion problem give values of the current drive parameter $J/P_d$ which agree with numerical results, both relativistically and nonrelativistically.

† Physics Department, Auburn University, Auburn, AL 36849
†† Massachusetts Institute of Technology, Plasma Fusion Center Cambridge, MA 02139
††† National Magnetic Fusion Energy Computer Center, Lawrence Livermore National Laboratory, Livermore, CA 94550
†††† GA Technologies, P.O. Box 85608, San Diego, CA 92138, USA

Turning to ICRF heating, two new all-metal antenna designs will permit power flux up to 10 $kW/cm^2$. A full wave solution to the magnetosonic wave equation, based on the parabolic method, yields cylindrical convergence and treats the diffraction limitation on intensity correctly. Mode conversion with energy absorption has been added to the BALDUR ICRF modeling code. A Fokker-Planck treatment of high energy ion tail formation by ICRF finds that enhanced thermonuclear reactivity can occur.

## I. LOWER HYBRID HEATING

### Theoretical Model for Current Ramp-up

It has been demonstrated that lower hybrid waves can be used to ramp up the plasma current.[1] Of particular interest is the fraction of input rf power, $P_{in}$, which goes into the poloidal magnetic field, $P_{field} = 1/2\, d(LI^2)/dt$, where I is the plasma current and L is the total inductance. In general, the contribution to $P_{field}$ due to changes in the internal inductance is small. The ratio of $P_{field}$ to $P_{in}$ is plotted versus the input power for a given series of PLT runs in Fig. 1. The lower hybrid waves are injected into a plasma with a decaying current. At the start of injection, the initial current ranges from 160 to 220 kA with the majority of the runs at an initial current of approximately 180 kA. The waveguide phasing is 60° for all the data shown.

The modeling code contains the following physics: The wave energy is propagated in the ray approximation using a warm plasma, electromagnetic dispersion relation. Toroidal effects on the ray propagation are included in the small aspect ratio limit. The waves exchange energy with the electrons and ions through the Landau interaction with distribution functions computed self-consistently from kinetic equations which include: quasilinear diffusion, collisional diffusion and drag, electric acceleration, and radial losses. Ion damping is negligible at the densities used in ramp-up but absorption by a hydrogen minority can be important at higher densities. The inductive electric field is determined self-consistently, including the effects of the strongly non-Maxwellian electron distribution function on the plasma conductivity. The electric field couples the flux diffusion equation to the Fokker-Planck equation for the electrons. The temperature and density profiles are not presently evolved in time.

For comparison with the experiments, the computed integral of $j \cdot E$ is equated with $P_{field}$. The code results for two values of $Z_{eff}$ are shown as solid lines in Fig. 1. The initial current is 180 kA, the average electron density is $3 \times 10^{12} cm^{-3}$, and the center temperature is 1.25 keV. For both $Z_{eff}$ cases approximately 40% of the input rf power is absorbed. Experimentally, it is found that a power of about 100 kW is required to maintain a steady-state current of 180 kA. This is in reasonable agreement with the $Z_{eff} = 4$ theoretical curve, while the $Z_{eff} = 1$ case requires approximately a factor of two less power. At higher power the experimentally determined efficiency of 12-14% is in better agreement with the $Z_{eff} = 1$ curve. A higher conversion efficiency, $P_{field}/P_{in}$, is obtained at higher power for $Z_{eff} = 4$ relative to $Z_{eff} = 1$, because at higher $Z_{eff}$ the back ohmic current opposing the ramp-up is reduced.

## Current-Drive Efficiency

Lower hybrid theory at MIT has focused on numerical and analytical solutions to the linearized steady-state two-dimensional Fokker-Planck equation for the resonant electrons in strong rf fields. The results show that there is an appreciable broadening of the resonant plateau in the direction perpendicular to the toroidal magnetic field and the tail perpendicular temperature $T_\perp >> T_B$, where $T_B = m_e v_t^2$ is the bulk temperature.

Analytically, for the nonrelativistic case and ion charge $Z_i = 1$, when D is constant for $v_1 \le v_\| \le v_2$ where $v_1(v_2)$ is the low (high) velocity boundary of the resonant domain, it is found that there are many more particles in the plateau, carrying the current, than estimated by 1D theory.[2] The ratio of the 2D current to the 1D current and $T_\perp/T_B$ are given by:

$$J_2/J_1 = v_1 v_2 [\pi \ln(v_2/v_1)/(v_2^2 - v_1^2)]^{1/2} = \pi T_\perp/2T_B \quad .$$

The figure of merit $J/P_d$ increases by a factor of 3, compared with the 1D theory and is given by: $J/P_d = (v_2^2 - v_1{}^2)/[2\ln(v_2/v_1)]$, where the current density J and the power dissipated $P_d$ are in units of $env_t$ and $m_e n v_t^2 \nu$ respectively. Here $\nu = 4\pi e^4 \, n(\ln\Lambda)/m_e^2 v_t^3$. This is in excellent agreement with the numerical result and explains the numerically found 2D enhancement.[3]

In accounting for relativistic effects, an analytic treatment based on a method of moments is developed where the relativistic Fokker-Planck equation for energetic electrons colliding with a thermal background of electrons and ions is used.[4] The moment equations yield the evolution equations of the average energy, momentum, and current of the energetic electrons. For the steady state with LH diffusion the figure of merit as well as the average perpendicular energy are given by:

$$(J/P_d)_R = [(\varepsilon+1)^2 - 1]/[(\varepsilon+1)^{3/2}(\varepsilon+2+Z_i)^{1/2}],$$

where the subscript R means that $J$ is in units of $enc$, $P_d$ is in units of $\nu_c mc^2 n$ ($\nu_c = \nu v_t^3/c^3$), and $\varepsilon = \gamma - 1$ is the kinetic energy (in units of $mc^2$) of the current carrying electrons; and

$$q_\perp^2[q_\perp^2 + (q_\perp^4 + 16q_\perp^2 + 16)^{1/2}] = 8(\gamma^2 - 1 - q_\perp^2) ,$$

where $q_\perp = v_\perp\gamma/c$, $v_\perp^2$ being a measure of the average perpendicular energy. The numerical results indicate a significant enhancement of the perpendicular temperature as well as of the radial one. For example, for a spectrum located between the parallel wave numbers 1.4 and 5, the current generated, power dissipated and the maximum perpendicular temperature, for Alcator C parameters, are 137 kA, 263 kW, and 130 keV respectively. A good agreement between the numerical results for the perpendicular temperature and the analytic, relativistic theory has been found. Relativity and the location of the spectrum affect significantly the current generated and power dissipated.

The numerical work has utilized an adaptive time-step, $\Delta t$, selection called Aggressive Alternating-Direction-Implicit (AADI) procedure. The asymptotic state for $f$ is achieved by using as few time steps as possible consistent with stability of the solution. A residue $\varepsilon$ is defined as $\varepsilon = (\partial f/\partial\tau)_{max}$, where max refers to the entire $v_\parallel(p_\parallel)$, $v_\perp(p_\perp)$ mesh. As long as $\varepsilon$ decreases, the solution is considered acceptable up to that "time" level and $\varepsilon$ is saved for future comparison. $\Delta t$ is gradually increased until $\varepsilon$ no longer decreases. An increase in $\varepsilon$ indicates the onset of numerical instability. The time step which is on the verge of instability is followed by a smaller $\Delta t$ which is intended to allow the solution to stabilize itself.

## II. ICRF HEATING

### ICRF Antennas

The radiation resistance of an ICRF antenna in a large tokamak can be computed from straightforward arguments.[5] Let the antenna size be large compared to the density decay distance in the plasma scrape-off layer. Then poloidal and parallel wave numbers can be ignored, a slab model is appropriate, and the magnetosonic wave equation takes the simple form:

$$(d^2E_\theta/dx^2) + (\omega^2/V_A^2)E_\theta = 0 \quad ; \quad k_o^2 = \omega^2/V_A^2 = \omega^2\ 4\pi nM/B^2 \quad .$$

Define $x_o$ as the position at which $k_o\ n/n' = 1$. The plasma surface impedance $\eta_s$ is then $\eta_s = \eta_o\ C(\omega/k_oc)_{x_o}$ where C lies in the range $1.2 < C < \pi$ depending on the details of the density profile.[5] Normally, $\eta_s << \eta_o$ and the Poynting flux into the plasma is $P = H_z^2\eta_s$ where $H_z$ is the impressed magnetic field computed as if a perfectly conducting surface existed at $x_o$.

Two promising ICRF antennas designs have been identified. Both ICRF antennas are versions of narrow-gap all-metal cavities with a moderate $Q \approx 15$ and have a modular construction which can be simply bolted on to a large port. The first design [5], carried out for the big-Dee Doublet III, consists of a shallow box with a novel active element which simultaneously functions as a coil and as a capacitor. The second[6], is a quarter wave segment of reentrant waveguide which acts as a loaded resonator. Both achieve perfect matching to transmission lines and radiate 10 $kW/cm^2$.

ICRF antennas generally have Faraday shields to eliminate the parallel electric field and to exclude neutral particles and radiation from the driven elements. These functions are aided by Faraday shield designs with narrow gaps. But the gaps cannot be too narrow or the rf magnetic field will not penetrate through them. The criterion[7] that magnetic shielding be negligible is $\pi\Delta y \ell / Lg \lesssim 0.3$, where $\Delta y$ denotes the poloidal periodicity length, $\ell$ the length of the narrow gap in the poloidal plane, g the gap spacing and L the length of a Faraday shield element along the toroidal field.

Propagation of Magnetosonic Waves

Let us turn to propagation of magnetosonic waves from the periphery to the center of a tokamak plasma. Qualitatively, the large decrease in Alfvén speed induces a cylindrical convergence of wave power into a focal spot where intensity is limited by diffraction. Ray tracing wave propagation algorithms cannot treat diffraction phenomena. This has motivated us to develop a new wave propagation algorithm based on the parabolic approximation to the wave equation. The new algorithm not only treats diffraction correctly, but is also more computationally efficient than ray-tracing techniques. Furthermore, it provides the electric field amplitudes and polarization needed to implement Fokker-Planck calculations of ion velocity distributions, and, via fast Fourier transforms, gives the incident Fourier amplitudes for mode conversion equations.

Our current code models the minority hydrogen/second harmonic deuterium heating in a cylindrical tokamak equilibrium, but it is readily generalized to treat other schemes by changes in the dielectric tensor elements. The algorithm divides the tokamak into two regions: an inner uniform-density region and an outer region where the parabolic approximation[8,9] is used. This approximation is based on the assumption that the wave propagates primarily in the radial direction, i.e., $\partial/\partial r \gg 1/r\ \partial/\partial\theta$. Under this assumption, the propagation is described by a single partial differential equation for $E_\theta$:

$$\frac{\partial}{\partial r}\frac{1}{r}\frac{\partial}{\partial r}\left(rE_\theta\right) + k_\theta^2 E_\theta - \frac{2i\omega}{\Omega r^2}\frac{\partial E_\theta}{\partial \theta} + \frac{1}{r^2}\frac{\partial^2 E_\theta}{\partial \theta^2} = 0 \quad , \qquad (1)$$

where $k_\sigma^2 = \omega^2/V_A^2$ and $V_A$ denotes the Alfvén speed and $\Omega$ the ion cyclotron frequency. By factoring out the rapidly varying cylindrical waveform from $E_\theta$, i.e., $E_\theta(r,\theta) = e(r)\ \psi(r,\theta)$, Eq. (1) is reduced to a parabolic equation for the slowly varying amplitude function, $\phi(r,\theta)$. The cylindrical waveform, $e(r)$, consists of generalized Hankel-type functions obtained by integrating the first two terms in Eq. (1) with $E_\theta$ replaced by $e(r)$. Amplitudes of the incoming and outgoing waves are determined by the launching structure, boundary condition at the conducting walls, and transmission and reflection coefficients associated with the mode conversion/cyclotron absorption layer. Analytic full wave solutions in the inner uniform density, strong focussing region are readily obtained since gradients in equilibrium quantities may be neglected in these regions. Fast Fourier transforms are utilized to match these solutions to the parabolic solutions and to the mode conversion/absorption layer.

Mode Conversion Processes During ICRF Heating of Tokamak Plasmas

In second harmonic and minority species approaches to ICRF heating a wave-particle interaction zone occurs where various plasma resonance conditions are satisfied. The wave in this region must be treated with kinetic theories which include linear and quasilinear effects. Near the locations of the resonances ($k \to \infty$) and cutoffs ($k \to 0$), the variation of the wave length is rapid so that the WKB approximation is no longer valid. Moreover, kinetic effects will introduce finite temperature plasma waves.

This leads to the possibility of mode conversion phenomenon where the dispersion properties of the cold plasma and kinetic waves coalesce in both real ($\underline{r}$) and ($\underline{k}$) space. To simplify the complex nature of the kinetic theory, only the fast wave and the ion Bernstein wave are included in the solution. Moreover, since the cutoff and mode conversion layers are essentially vertical slabs, a one-dimensional approximation in the direction of the major radius is used in the mode conversion region. The mode conversion calculation has been linked with the ray tracing and transport codes to simulate ICRF heating of tokamak plasmas.

The general one-dimensional, fourth order mode conversion equation, including absorption[10], is solved using the Green's function technique to obtain the tunnelling (T), relection (R), and mode conversion (C) coefficients. The value of these coefficients depends on the direction of the incoming wave (either from the cutoff region or the mode conversion region). When absorption is included in the calculations, numerical solutions for the coefficients are necessary. As an example, new results for the coefficients in the second harmonic case are summarized in Table I, where $\alpha_{c1} = 0.16\eta^{-2/3}e^{-2\eta}$, $\alpha_{c2} = 0.9\eta^{-0.42}$, $\rho = e^{\eta}\mu^4/\pi(1+\gamma)^{1/2}|\Gamma[(3/4)+(i\eta/\pi)]|^2$, $\eta = \pi(1+\gamma)/2\lambda^2$ and the conversion of energy gives $|T_k|^2 + |R_k|^2 + \rho|E_k|^2 + E_{abs} = 1$. (See Ref. 10 for the definition of $\lambda$, $\gamma$, $\mu$.)

TABLE I

Transmission, Reflection, and Mode Conversion Coefficients

for Second Harmonic Heating

| Case | Transmission | Reflection | Conversion |
| --- | --- | --- | --- |
| Fast wave; High Field Incidence | $\|T_1\|^2 = e^{-2\eta}$ | $\|R_1\|^2 = 0$ | $\rho\|C_1\|^2 = (1-e^{-2\eta})e^{-\alpha_{c1}\kappa^2}$ |
| Fast wave; Low Field Incidence | $\|T_2\|^2 = e^{-2\eta}$ | $\|R_2\|^2 = (1-e^{-2\eta})^2 e^{-2\kappa^2}$ | $\rho\|C_2\|^2 = e^{-2\eta}(1-e^{-2\eta})\ e^{-2\alpha_{c2}\kappa^2}$ |
| Ion Bernstein Wave; High Field Incidence | $\|T_3\|^2 = 0$ | $\|R_3\|^2 = e^{-4\eta-2\alpha_{R3}\kappa^2}$ | $\|C_3^+\|^2/\rho = (1-e^{-2\eta})e^{-2\alpha_{c1}\kappa^2}$<br>$\|C_3^-\|^2/\rho = e^{-2\eta}(1-e^{-2\eta})e^{-2\alpha_{c2}\kappa^2}$ |

Fokker-Planck Calculations of Fusion Reactivity

We have examined fusion reactivity enhancement by ICRF heating in large tokamaks using a new bounce-averaged, two-dimensional Fokker-Planck code including a general quasilinear operator. The heating is applied to only one plasma species. The remaining species are represented by fixed temperature Maxwellians. The reactivity enhancement is characterized by dividing the resulting bounce-averaged fusion reaction rate by that obtained from an equivalent Maxwellian distribution: The equivalence here is defined by requiring the collisional power transfer to the remaining species to equal the applied rf power.

We have considered the $\omega = 2\ \omega_{cd}$ case in detail. The solid lines in Fig. 2 show results of a parameter survey of the $\langle\sigma v\rangle$-enhancement obtained by varying the electron density and the background electron and tritium temperature for a 50-50 DT plasma with an absorbed rf power of 0.5 $W/cm^3$. The rf perpendicular wavenumber is chosen according to the cold plasma dispersion relation with $n_\parallel = 2$. Large fusion reaction rate enhancements, greater than 3, are obtained at the lower densities and temperatures. In order for the $\langle \sigma v \rangle$-enhancement to impact the overall power balance, the Q (fusion/rf power) must also be appreciable. For Q = 0.5 and $\langle \sigma v \rangle$-enhancement greater than 2, the additional fusion power output is 25% of the input RF power, and thus is a significant factor in the power balance. For Q = 0.5 and $T_e = T_T = 6$ keV the $\langle \sigma v \rangle$-enhancement remains approximately equal to 2.0 as the rf power and density are scaled together up to 2 $W/cm^3$ and $2 \times 10^{14} cm^{-3}$.

The ion tail formation gives additional velocity space average results. The poloidal density variation associated with build up of fast ion banana tips in the resonance layer is found to be up to 5% over the range of parameters covered by Fig. 2. The poloidal variation of fusion reactivity is found as high as a factor of 2 at the lowest temperature; this effect decreases with temperature. Going to higher power and proportionately greater density results in approximately the same poloidal variation as a function of temperature.

ACKNOWLEDGMENTS

Work performed under the auspices of the U.S. Dept. of Energy by Princeton University, Contract No. DE-AC02-76-CHO-3073, by M.I.T., Contract No. DE-AC02-78ET-51013, by Lawrence Livermore National Laboratory Contract No. W-7405-ENG-48, and by GA Technologies Inc. Contract No. DE-AT03-84ER53158. Work at M.I.T. was also supported by NSF Grant ECS 82-13430.

# REFERENCES

[1]HOOKE, W., Plasma Physics and Controlled Nuclear Fusion 26 (1984) 133.

[2]FISCH, N. J., Phys. Rev. Lett. 41 (1978) 873.

[3]KARNEY, C. F. F., FISCH, N. J., Phys. Fluids 22 (1979) 1817.

[4]HIZANIDIS, K., MOLVIG, K., SWARTZ, K., J. Plasma Phys. 32 (1983) 223.

[5]PERKINS, F. W., KLUGE, R. F., IEEE Trans. Plasma Science, PS-12, (1984) 161.

[6]PERKINS, F. W., "Reentrant Waveguide Antennas for ICRF Heating of Large Tokamaks" in Proc. 4th Int. Symposium on Heating in Toroidal Plasmas, Vol. 2, (Rome, 1984).

[7]PERKINS, F.W. "Magnetic Shielding by a Faraday Shield", in Proc. 4th Int. Symposium on Heating in Toroidal Plasmas, Vol. 2, 1174 (Rome, 1984).

[8]TAPPERT, F., J. Opt. Soc. Am., 66 (1976) 1368.

[9]PHILLIPS, C. K., PERKINS, F. W., HWANG, D. W., Proc. 4th Int. Symposium on Heating in Toroidal Plasmas, Vol. 1, 457 (Rome, 1984).

[10]SWANSON, D. G., Nucl. Fusion 20 (1980) 949; Phys. Fluids 24 (1981) 2035.

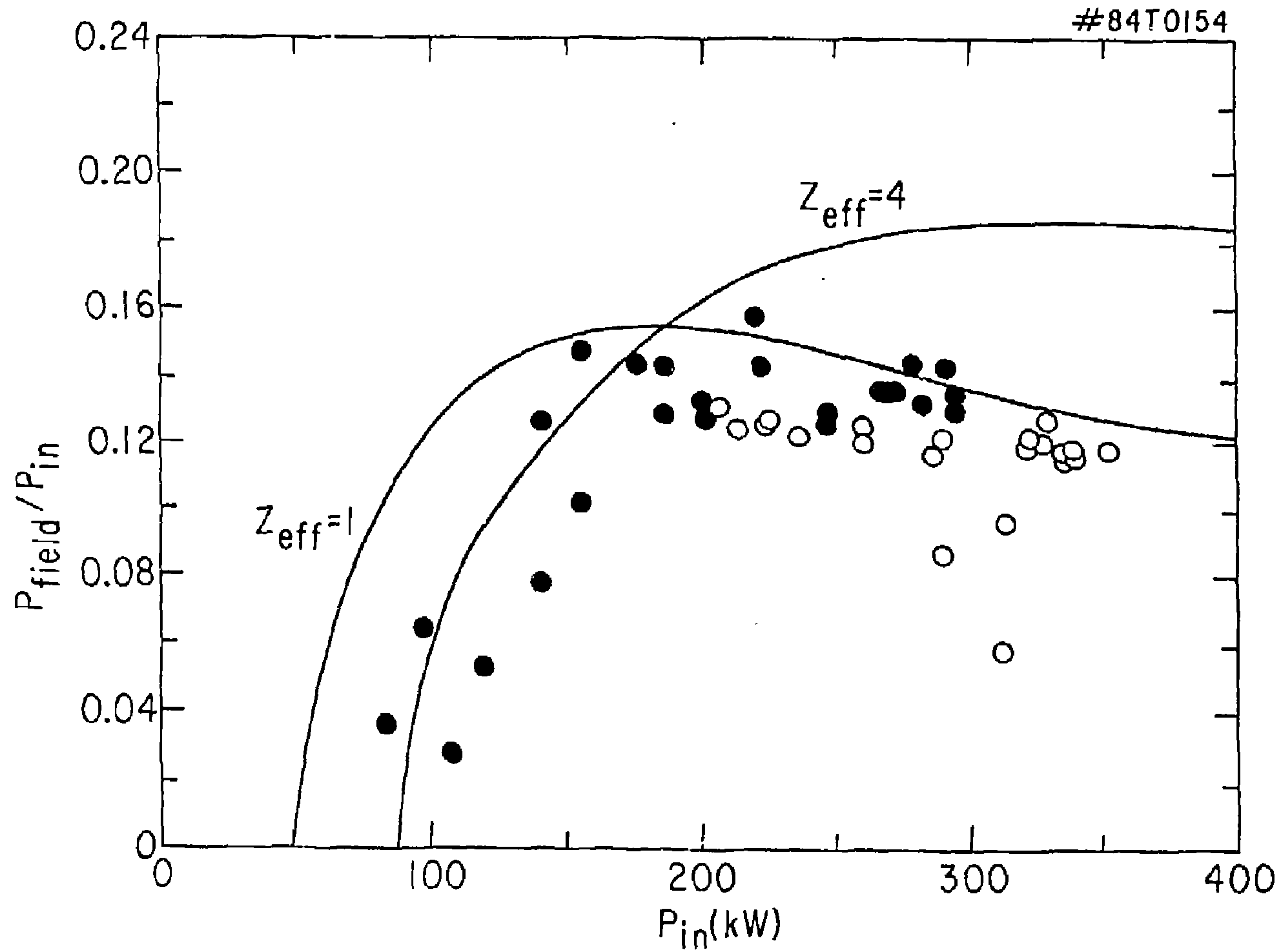


FIG. 1. Theoretical (solid curves) and experimental values for the current ramp-up efficiency in PLT. Solid (open) points are from discharges with line average density $3.1-3.3 \times 10^{12} cm^{-3}$ ($3.4-3.6 \times 10^{12} cm^{-3}$)

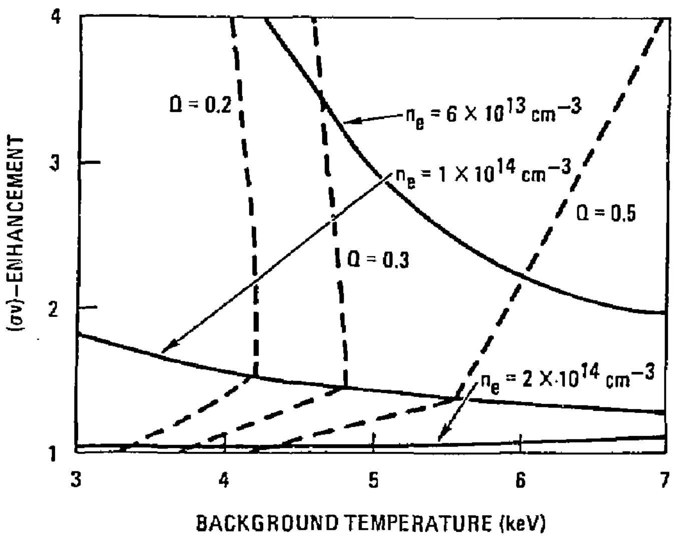


FIG. 2. <σv>-enhancement versus background temperature, with $n_e$ as parameter (solid line). The dashed line connects constant Q points.

EXTERNAL DISTRIBUTION IN ADDITION TO UC-20

Plasma Res Lab, Austra Nat'l Univ, AUSTRALIA
Dr. Frank J. Paoloni, Univ of Wollongong, AUSTRALIA
Prof. I.R. Jones, Flinders Univ., AUSTRALIA
Prof. M.H. Brennan, Univ Sydney, AUSTRALIA
Prof. F. Cap, Inst Theo Phys, AUSTRIA
Prof. Frank Verheest, Inst theoretische, BELGIUM
Dr. D. Palumbo, Dg XII Fusion Prog, BELGIUM
Ecole Royale Militaire, Lab de Phys Plasmas, BELGIUM
Dr. P.H. Sakanaka, Univ Estadual, BRAZIL
Dr. C.R. James, Univ of Alberta, CANADA
Prof. J. Teichmann, Univ of Montreal, CANADA
Dr. H.M. Skarsgard, Univ of Saskatchewan, CANADA
Prof. S.R. Sreenivasan, University of Calgary, CANADA
Prof. Tudor W. Johnston, INRS-Energie, CANADA
Dr. Hannes Barnard, Univ British Columbia, CANADA
Dr. M.P. Bachynski, MPB Technologies, Inc., CANADA
Chalk River, Nucl Lab, CANADA
Zhengwu Li, SW Inst Physics, CHINA
Library, Tsing Hua University, CHINA
Librarian, Institute of Physics, CHINA
Inst Plasma Phys, Academia Sinica, CHINA
Dr. Peter Lukac, Komenskeho Univ, CZECHOSLOVAKIA
The Librarian, Culham Laboratory, ENGLAND
Prof. Schatzman, Observatoire de Nice, FRANCE
J. Radet, CEN-BP6, FRANCE
AM Dupas Library, AM Dupas Library, FRANCE
Dr. Tom Mual, Academy Bibliographic, HONG KONG
Preprint Library, Cent Res Inst Phys, HUNGARY
Dr. S.K. Trehan, Panjab University, INDIA
Dr. Indra Mohan Lal Das, Banaras Hindu Univ, INDIA
Dr. L.K. Chavda, South Gujarat Univ, INDIA
Dr. R.K. Chhajlani, Vikram Univ. INDIA
Dr. B. Dasgupta, Saha Inst, INDIA
Dr. P. Kaw, Physical Research Lab, INDIA
Dr. Phillip Rosenau, Israel Inst Tech, ISRAEL
Prof. S. Cuperman, Tel Aviv University, ISRAEL
Prof. G. Rostagni, Univ Di Padova, ITALY
Librarian, Int'l Ctr Theo Phys, ITALY
Miss Clelia De Palo, Assoc EURATOM-ENEA, ITALY
Biblioteca, del CNR EURATOM, ITALY
Dr. H. Yamato, Toshiba Res & Dev, JAPAN
Direc. Dept. Lg. Tokamak Dev. JAERI, JAPAN
Prof. Nobuyuki Inoue, University of Tokyo, JAPAN
Research Info Center, Nagoya University, JAPAN
Prof. Kyoji Nishikawa, Univ of Hiroshima, JAPAN
Prof. Sigeru Mori, JAERI, JAPAN
Library, Kyoto University, JAPAN
Prof. Ichiro Kawakami, Nihon Univ, JAPAN
Prof. Satoshi Itoh, Kyushu University, JAPAN
Dr. D.I. Choi, Adv. Inst Sci & Tech, KOREA
Tech Info Division, KAERI, KOREA
Bibliotheek, Fom-Inst Voor Plasma, NETHERLANDS
Prof. B.S. Liley, University of Waikato, NEW ZEALAND
Prof. J.A.C. Cabral, Inst Superior Tecn, PORTUGAL
Dr. Octavian Petrus, ALI CUZA University, ROMANIA
Prof. M.A. Hellberg, University of Natal, SO AFRICA
Dr. Johan de Villiers, Plasma Physics, Nucor, SO AFRICA
Fusion Div. Library, JEN, SPAIN
Prof. Hans Wilhelmson, Chalmers Univ Tech, SWEDEN
Dr. Lennart Stenflo, University of UMEA, SWEDEN
Library, Royal Inst Tech, SWEDEN
Centre de Recherchesen, Ecole Polytech Fed, SWITZERLAND
Dr. V.T. Tolok, Kharkov Phys Tech Ins, USSR
Dr. D.D. Ryutov, Siberian Acad Sci, USSR
Dr. G.A. Eliseev, Kurchatov Institute, USSR
Dr. V.A. Glukhikh, Inst Electro-Physical, USSR
Institute Gen. Physics, USSR
Prof. T.J.M. Boyd, Univ College N Wales, WALES
Dr. K. Schindler, Ruhr Universitat, W. GERMANY
Nuclear Res Estab, Julich Ltd, W. GERMANY
Librarian, Max-Planck Institut, W. GERMANY
Bibliothek, Inst Plasmaforschung, W. GERMANY
Prof. R.K. Janev, Inst Phys, YUGOSLAVIA